

Family of Heterometallic Semicircular Mn^{III}₂Ln^{III}₃ Strands

Muhammad Nadeem Akhtar, Yan-Zhen Zheng, Yanhua Lan, Valeriu Mereacre, Christopher E. Anson, and Annie K. Powell*

Institut für Anorganische Chemie der Universität Karlsruhe (TH), Karlsruhe Institute of Technology, Engesserstrasse 15, 76131 Karlsruhe, Germany

Received January 14, 2009

A series of heterometallic complexes of formula [Mn^{III}₂Ln^{III}₃-(bdeaH)₃(bdea)₂(piv)₃]·MeCN, where bdeaH₂ = *N*-butyldiethanolamine, piv = pivalate, and Ln = Y (1), Tb (2), Dy (3), Ho (4), and Er (5), has been prepared. 1–5 are isostructural, with the metal centers forming a novel semicircular Ln^{III}–Mn^{III}–Ln^{III}–Mn^{III}–Ln^{III} strand. Only 2 and 3 exhibit slow relaxation of the magnetization, suggesting that the highly anisotropic Ln^{III} ions (Tb^{III} and Dy^{III}) are essential for an energy barrier to spin reversal.

The search for new generations of single-molecule magnets (SMMs)¹ aims to find systems that can be developed for future applications in quantum computation and data storage.² Until recently, most investigations focused on using 3d transition-metal ions as the source of paramagnetic ions to make SMMs, with a particular emphasis on manganese clusters incorporating the Mn^{III} ion, which usually has a uniaxial anisotropy in its high spin state. For compounds with non-zero spin ground states and a negative zero-field-splitting parameter for the entire molecule, *D*, an energy barrier to the reversal of the molecular spin in the ground state (*S*_T) should be generated in the form of $\Delta = |D|S_T^2$ for integer spin and $|D|(S_T^2 - 1/4)$ for half-integer spin, although a recent reappraisal of this suggests that the relationship is linearly dependent on the spin *S*_T,³ in turn directing research toward increasing the anisotropy in new systems.

Until recently, manganese clusters showed the slowest relaxation times for SMMs, but with the discovery of lanthanide-based SMMs, even longer times can be measured. In fact, the spin-reversal mechanism in pure lanthanide systems is different from that in operation for the 3d SMMs mentioned above, and according to some previously reported results,^{4,5} the energy barrier of spin reversal in lanthanide-based SMMs mainly arises from the zero-field splitting of the ground states of angular momentum (*J*) with (2*J* + 1)-fold degeneracy.⁶ Unlike in the case of the *D* value, which is mainly governed by the single-ion anisotropy in concert with the exchange coupling between metal centers, the energy differences between the sublevels of *J* are mainly controlled by the ligand field.^{4–6} Although the two mechanisms of slow relaxation are different, it is of interest to see what happens when these effects are combined in one molecule, which is a significant motivation in the fabrication of 3d–4f heterometallic clusters.

The natural choice of the 3d metal ion would be Mn^{III} for the reasons already outlined. We and other groups have investigated clusters containing Mn^{III} and Ln^{III} ions, such as Mn₂Dy₂,^{7a} Mn₆Dy₆,^{7b} Mn₁₁Dy₄,^{7c} Mn₁₁Gd₂,^{8a} Mn₅Ln₄,^{8b} Mn₁₀Ln₂ (Ln = Pr and Nd),^{8c} and Mn₁₁Eu₄.^{8c} Among them, Mn₅Dy₄^{8b} has the highest energy barrier for 3d–4f SMMs at 38.6 K. Although this value is less than those of pure Mn^{III}- or Ln^{III}-based SMMs, it indicates a promising avenue toward producing SMMs with higher energy barriers, with the challenge being to discover how the interplay of the mixed 3d and 4f ions can be optimized to achieve this goal. At present, many parameters need to be explored and a useful way forward is to compare properties for an isostructural series of compounds, as we show here.

* To whom correspondence should be addressed. E-mail: powell@aoc.uni-karlsruhe.de. Fax: +49-721-6088142.

- (1) See reviews: (a) Christou, G.; Gatteschi, D.; Hendrickson, D. N.; Sessoli, R. *MRS Bull.* **2000**, *25*, 66. (b) Gatteschi, D.; Sessoli, R. *Angew. Chem., Int. Ed.* **2003**, *43*, 268. (c) Aromí, G.; Brechin, E. K. *Struct. Bonding (Berlin)* **2006**, *122*, 1.
- (2) Leuenberger, M. N.; Loss, D. *Nature* **2001**, *410*, 789.
- (3) Waldmann, O. *Inorg. Chem.* **2007**, *46*, 10035.
- (4) (a) Ishikawa, N.; Sugita, M.; Wernsdorfer, W. *J. Am. Chem. Soc.* **2005**, *127*, 3650. (b) Ishikawa, N.; Sugita, M.; Wernsdorfer, W. *Angew. Chem., Int. Ed.* **2005**, *44*, 2931. (c) Takamatsu, S.; Ishikawa, T.; Koshihara, S.-y.; Ishikawa, N. *Inorg. Chem.* **2007**, *46*, 7250.
- (5) (a) Tang, J.; Hewitt, I.; Madhu, N. T.; Chastanet, G.; Wernsdorfer, W.; Anson, C. E.; Benelli, C.; Sessoli, R.; Powell, A. K. *Angew. Chem., Int. Ed.* **2006**, *45*, 1729. (b) Luzon, J.; Bernot, K.; Hewitt, I. J.; Anson, C. E.; Powell, A. K.; Sessoli, R. *Phys. Rev. Lett.* **2008**, *100*, 247205. (c) Chibotaru, L. F.; Ungur, L.; Soncini, A. *Angew. Chem., Int. Ed.* **2008**, *47*, 4126.

- (6) Benelli, C.; Gatteschi, D. *Chem. Rev.* **2002**, *102*, 2369.
- (7) (a) Mishra, A.; Wernsdorfer, W.; Parson, S.; Christou, G.; Brechin, E. *Chem. Commun.* **2005**, 2086. (b) Zaleski, C.; Depperman, E.; Kampf, J.; Kirk, M.; Pecoraro, V. *Angew. Chem., Int. Ed.* **2005**, *44*, 3912. (c) Mishra, A.; Wernsdorfer, W.; Abboud, K.; Christou, G. *J. Am. Chem. Soc.* **2004**, *126*, 15648.
- (8) (a) Mereacre, V.; Ako, A. M.; Clérac, R.; Wernsdorfer, W.; Filoti, G.; Bartolomé, J.; Anson, C. E.; Powell, A. K. *J. Am. Chem. Soc.* **2007**, *129*, 9248. (b) Mereacre, V.; Ako, A. M.; Clérac, R.; Wernsdorfer, W.; Hewitt, I. J.; Anson, C. E.; Powell, A. K. *Chem.—Eur. J.* **2008**, *45*, 707. (c) Mereacre, V.; Prodius, D.; Ayuk, A. M.; Kaur, N.; Lipkowsky, J.; Simmons, C.; Dalal, N.; Geru, I.; Anson, C. E.; Powell, A. K.; Turta, C. *Polyhedron* **2008**, *27*, 2459.

Following our previous work on the construction of pure 3d transition-metallic clusters such as Mn_4 , Fe_7 , and Fe_8 in systems incorporating the ligand *N*-butyldiethanolamine (bdeaH_2),⁹ we now are able to expand its use in synthesizing 3d–4f heterometallic clusters with the aid of pivalic acid (*piv*) as the coligand. We have already reported that the reaction of light lanthanide ions resulted in tetranuclear $\text{Mn}^{\text{III}}_2\text{Ln}^{\text{III}}_2$ ($\text{Ln} = \text{La}, \text{Ce}, \text{Pr}, \text{and Nd}$) clusters.¹⁰ We now report that using the heavier lanthanides in this reaction system¹¹ results in a family of isostructural compounds $[\text{Mn}^{\text{III}}_2\text{Ln}_3(\text{bdeaH})_3(\text{bdea})_2(\text{piv})_8] \cdot \text{MeCN}$ [$\text{Ln} = \text{Y}$ (**1**), Tb (**2**), Dy (**3**), Ho (**4**), and Er (**5**)] in which the metals form an unprecedented semicircular $\text{Ln}^{\text{III}}\text{—Mn}^{\text{III}}\text{—Ln}^{\text{III}}\text{—Mn}^{\text{III}}\text{—Ln}^{\text{III}}$ strand.

Single-crystal X-ray diffraction studies¹² reveal that **1–5** are isomorphous, and only the structure of **3** will be described here. The metal centers form an alternating $\text{Dy}^{\text{III}}\text{—Mn}^{\text{III}}\text{—Dy}^{\text{III}}\text{—Mn}^{\text{III}}\text{—Dy}^{\text{III}}$ strand, in which adjacent pairs of metals are bridged by two alkoxide O atoms from two different bdea^{2-} (for the central portion) or bdeaH^- (for the outer metals) ligands and one *syn*, *syn*-carboxylate bridge. The $\text{Mn}^{\text{III}}\cdots\text{Dy}^{\text{III}}$ distances range from 3.3521(8) to 3.3902(8) Å. This strand of five metals is pulled into a semicircular shape by the fifth bdeaH^- ligand, whose oxygens, O(9) and O(10), each bridge two outer pairs of metals (Figure 1). With the exception of this ligand, the molecule has idealized C_{2v} symmetry; the pentanuclear core is close to planar, with Mn(1) and Mn(2) displaced by +0.654

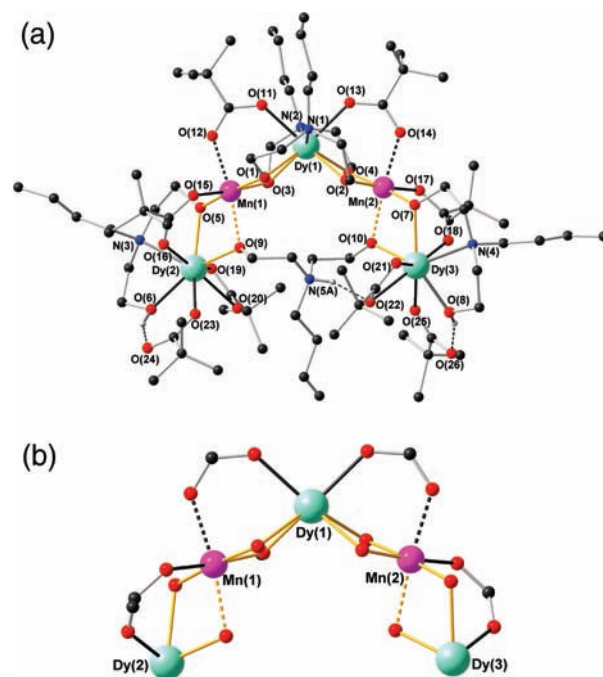


Figure 1. View of complex **3** (a) and the semicircular $\text{Mn}^{\text{III}}_2\text{—Dy}^{\text{III}}_3$ strand (b). Color code: Mn, pink; Dy, green; N, blue; O, red; C, black. The elongated Jahn–Teller axes of Mn^{III} ions are shown as dashed lines.

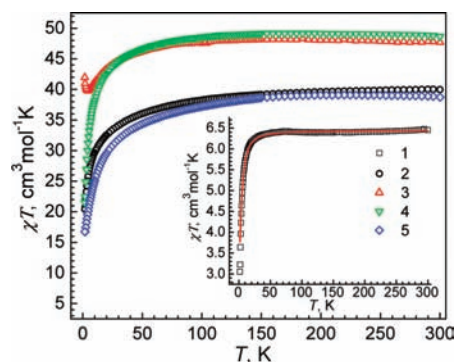


Figure 2. Plots of χT vs T at an applied field of 0.1 T for **2–5**. Inset: Plot of χT vs T at an applied field of 0.1 T for **1**. Solid red line: Fitted by the model of a single Mn^{III} ion.

- (9) (a) Ayuk, A. M.; Mereacre, V. M.; Hewitt, I. J.; Clerac, R.; Lecren, L.; Anson, C. E.; Powell, A. K. *J. Mater. Chem.* **2006**, *15*, 2579. (b) Ayuk, A. M.; Waldmann, O.; Mereacre, V.; Klöwer, F.; Hewitt, I.; Anson, C. E.; Gudel, H. U.; Powell, A. K. *Inorg. Chem.* **2007**, *46*, 756.
- (10) Akhtar, M. N.; Lan, Y.; Mereacre, V.; Clérac, R.; Anson, C. E.; Powell, A. K. *Polyhedron* **2008**, doi:10.1016/j.poly.2008.10.062.
- (11) Synthesis of **1**: A solution of bdeaH_2 (0.64 g, 4.0 mmol) in 10 mL of MeCN and $\text{Y}(\text{NO}_3)_3 \cdot 6\text{H}_2\text{O}$ (0.22 g, 0.5 mmol) was added to a stirred solution of $\text{Mn}(\text{OAc})_2 \cdot 4\text{H}_2\text{O}$ (0.12 g, 0.5 mmol) and pivalic acid (0.20 g, 2.0 mmol) in 10 mL of MeCN to give a dark-brown solution. After 48 h, brown crystals were collected by filtration and washed with acetonitrile. Yield: 25% (based on Mn). Anal. Calcd for $\text{C}_{82}\text{H}_{163}\text{Mn}_2\text{Y}_3\text{N}_6\text{O}_{26}$ (**1**): C, 48.62; H, 8.11; N, 4.15. Found: C, 48.45; H, 7.95; N, 4.08. IR (KBr, cm^{-1}): 3425 (b), 3073 (m), 2959 (vs), 2928 (s), 1580 (s), 1550 (vs), 1482 (vs), 1411 (vs), 1374 (s), 1227 (s), 1088 (s), 907 (m), 792 (w), 746 (w), 638 (s), 606 (m), 550 (w). Syntheses for **2–5**: Same as that for **1** but using $\text{Ln}(\text{NO}_3)_3 \cdot 6\text{H}_2\text{O}$ with $\text{Ln} = \text{Tb}, \text{Dy}, \text{Ho}, \text{and Er}$. Further details are given in the Supporting Information.
- (12) Crystal data for **1**: $\text{C}_{82}\text{H}_{163}\text{Mn}_2\text{Y}_3\text{N}_6\text{O}_{26}$, $M = 2025.79 \text{ g mol}^{-1}$, monoclinic, $P2_1/n$, $T = 100 \text{ K}$, $a = 17.3318(7) \text{ \AA}$, $b = 29.7220(12) \text{ \AA}$, $c = 20.4829(8) \text{ \AA}$, $\beta = 100.803(1)^\circ$, $V = 10364.5(7) \text{ \AA}^3$, $Z = 4$, $\rho_c = 1.298 \text{ g cm}^{-3}$, $\mu(\text{Mo K}\alpha) = 1.966 \text{ mm}^{-1}$; total/unique data 60 793/19 621, $R_{\text{int}} = 0.0671$, 1072 parameters, $wR2 = 0.1399$, $S = 1.034$ (all data), $R1 = 0.0524$ [12 470 with $I \geq 2\sigma(I)$], largest peak/hole $+0.81/-0.49 \text{ e \AA}^{-3}$. Crystal data for **3**: $\text{C}_{82}\text{H}_{163}\text{Dy}_3\text{Mn}_2\text{N}_6\text{O}_{26}$, $M = 2246.56 \text{ g mol}^{-1}$, monoclinic, $P2_1/n$, $T = 150 \text{ K}$, $a = 17.5013(6) \text{ \AA}$, $b = 29.8075(13) \text{ \AA}$, $c = 20.5822(7) \text{ \AA}$, $\beta = 100.699(3)^\circ$, $V = 10550.5(7) \text{ \AA}^3$, $Z = 4$, $\rho_c = 1.414 \text{ g cm}^{-3}$, $\mu(\text{Mo K}\alpha) = 2.398 \text{ mm}^{-1}$; total/unique data 72 230/22 433, $R_{\text{int}} = 0.0391$, 1063 parameters, $wR2 = 0.1380$, $S = 1.012$ (all data), $R1 = 0.0536$ [17 819 with $I \geq 2\sigma(I)$], largest peak/hole $+0.67/-2.38 \text{ e \AA}^{-3}$. Crystal data for **5**: $\text{C}_{82}\text{H}_{163}\text{Er}_3\text{Mn}_2\text{N}_6\text{O}_{26}$, $M = 2260.84 \text{ g mol}^{-1}$, monoclinic, $P2_1/n$, $T = 100 \text{ K}$, $a = 17.2846(4) \text{ \AA}$, $b = 29.7522(7) \text{ \AA}$, $c = 20.5363(5) \text{ \AA}$, $\beta = 100.764(1)^\circ$, $V = 10375.1(4) \text{ \AA}^3$, $Z = 4$, $\rho_c = 1.447 \text{ g cm}^{-3}$, $\mu = 2.704 \text{ mm}^{-1}$; total/unique data 64 453/23 388, $R_{\text{int}} = 0.0457$, 1079 parameters, $wR2 = 0.0936$, $S = 1.020$ (all data), $R1 = 0.0402$ [17 868 with $I \geq 2\sigma(I)$], largest peak/hole $+1.74/-0.70 \text{ e \AA}^{-3}$. Crystallographic data (excluding structure factors) for **1**, **3**, and **5** deposited as supplementary publication nos. CCDC 716071–716073. **2** and **4** were shown to be isomorphous to **1**, **3** and **5**. Crystal data for **2**: $a = 17.457(15) \text{ \AA}$, $b = 29.649(18) \text{ \AA}$, $c = 20.555(16) \text{ \AA}$, $\beta = 100.93(7)^\circ$, $V = 10446(13) \text{ \AA}^3$. Crystal data for **4**: $a = 17.361(3) \text{ \AA}$, $b = 29.762(3) \text{ \AA}$, $c = 20.574(4) \text{ \AA}$, $\beta = 100.888(7)^\circ$, $V = 10439(6) \text{ \AA}^3$.

and -0.705 \AA out of the Dy_3 plane. The bridging bdeaH^- ligand does not conform to the C_{2v} symmetry of the rest of the molecule, and in contrast to the other two bdeaH^- ligands, it is the central N atom that carries the proton rather than one of the alcohol arms. This ligand is 50:50 disordered, with the protonated nitrogen N(5) forming a hydrogen bond either to O(22) (as in Figure 1) or to O(20), the corresponding oxygen on the other side of the molecule. It should be noted that the Jahn–Teller axes of the two Mn^{III} ions are almost parallel, subtending an angle of 14.63° , with a $\text{Mn}^{\text{III}}\cdots\text{Mn}^{\text{III}}$ distance of 5.873 \AA . Moreover, the molecules are well separated within the crystal structure, and no intermolecular hydrogen bonds were observed in the crystal packing.

Direct current (dc) magnetic susceptibility data for compounds **1–5** were collected in the 1.8–300 K temperature range under a field of 0.1 T (Figure 2). For all five compounds, the χT product at 300 K is close to the expected value for two Mn^{III} ions and the three respective Ln^{III} cations. All of the χT products remain almost constant above 100 K, where they can be well

Table 1. Ground-State and Room Temperature χ Values for the Mn_2Ln_3 Core

compound	ground state of Ln	Curie constant for Ln	predicted χT ($\text{cm}^3 \text{mol}^{-1} \text{K}$)	observed χT ($\text{cm}^3 \text{mol}^{-1} \text{K}$)	Weiss constant θ^a (K)
Mn_2Y_3 (1)	diamagnetic	0	6.0	6.5	−1.17
Mn_2Tb_3 (2)	$^7\text{F}_6$	11.82	41.5	40.0	−4.91
Mn_2Dy_3 (3)	$^6\text{H}_{15/2}$	14.17	48.5	47.7	−1.47
Mn_2Ho_3 (4)	$^5\text{I}_8$	14.07	48.2	48.8	−2.66
Mn_2Er_3 (5)	$^4\text{I}_{15/2}$	11.48	40.5	38.7	−6.46

^a θ is obtained by fitting of the Curie–Weiss law from 100 to 300 K.

fitted by the Curie–Weiss law with results summarized in Table 1. However, even if the χT product decreases with a small negative Weiss constant, it is not possible to be sure that this behavior is associated with antiferromagnetic interactions within the complex due to the presence of strong spin–orbital coupling effects in these Ln^{III} ions.

The increase of χT of **3** below 5 K may indicate the presence of ferromagnetic interactions between spin carriers within the strand. However, the magnetic interactions of this series of compounds arise from the sum of interactions of $\text{Mn}^{\text{III}}\text{–Mn}^{\text{III}}$, $\text{Mn}^{\text{III}}\text{–Ln}^{\text{III}}$, and $\text{Ln}^{\text{III}}\text{–Ln}^{\text{III}}$ in addition to the intrinsic magnetic properties of the Ln^{III} ions, which hamper attempts to determine the exact constants of the magnetic interactions among them. Fortunately, insights can be gained by studying the Y^{III} analogue (**1**) in order to quantify the magnetic interactions between Mn^{III} ions. The compound can be first viewed as a dimer of Mn^{III} ions; the interaction (J) between Mn^{III} and Mn^{III} is calculated as $J/k_B = -0.31(1)$ K with $g = 2.08(1)$ (see Figure S1 in the Supporting Information). Alternatively, we can effectively regard compound **1** as containing only two isolated Mn^{III} ions. The spin Hamiltonian of a single Mn^{III} ion is given by

$$\hat{H} = D[\hat{S}_z^2 - \frac{1}{3}S(S+1)] + g\mu_B H \hat{S}$$

This model was able to reproduce the experimental data in the full temperature range with the incorporation of the mean-field approximation, χT . The best set of parameters found is $|D|/k_B = 4.2(3)$ K, $g = 2.074(1)$, and $|zJ|/k_B = 0.055(7)$ K with the sign of D probably negative given the nearly parallel elongated Jahn–Teller axes of the Mn^{III} ions.¹ The amplitude of the D value indicates that the magnetic anisotropy is large and the χT value suggests that the interactions between the two Mn^{III} ions are weak, which indicates that in the other compounds of this family the Mn^{III} ions are likely to contribute a large magnetic anisotropy with weak magnetic coupling between them.

The field dependence of the magnetization at low temperature for each of the compounds **1–5** shows a relative increase of the magnetization at low fields, followed by an almost linear increase without clear saturation up to 7 T, where it reaches 7.3, 19.1, 22.9, 24.6, and 21.0 μ_B for **1–5**, respectively (Figures S2–S6 in the Supporting Information). The non-overlapping M vs H/T curves unambiguously indicate significant magnetic anisotropy in these compounds (Figures S2–S6 in the Supporting Information).

As a result of the magnetic anisotropy present in these compounds, the alternating current (ac) susceptibility measurements were checked under zero dc fields. There is no out-of-

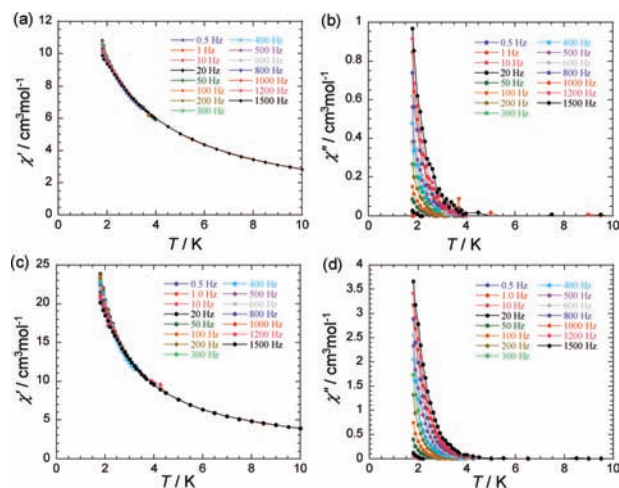


Figure 3. Temperature dependence of the in-phase (a and c for **2** and **3**, respectively) and out-of-phase (b and d for **2** and **3**, respectively) ac susceptibilities at the indicated frequencies.

phase signal shown above 1.8 K for compounds **1**, **4**, and **5**, while for **2** and **3**, out-of-phase signals are clearly detected (about 10% and 16% of the in-phase signal for **2** and **3**, respectively) below 4 K (Figure 3), supporting the conclusion that these compounds exhibit slow relaxation of the magnetization and are SMMs.

Since in this series of $\text{Mn}^{\text{III}}_2\text{Ln}^{\text{III}}_3$ compounds only **2** and **3** exhibit slow relaxation and no of out-of-phase signal is observed in compound **1**, it is impossible that slow relaxation originates from the Mn^{III} ions alone. Thus, we can conjecture that the slow relaxation arises either solely from the anisotropic Ln^{III} ions or from a combination of the Mn^{III} and Ln^{III} ions.

In summary, a family of heterometallic complexes with a semicircular $\text{Ln}^{\text{III}}\text{–Mn}^{\text{III}}\text{–Ln}^{\text{III}}\text{–Mn}^{\text{III}}\text{–Ln}^{\text{III}}$ strand is described. The observation of magnetic slow-relaxation behavior in **2** and **3** suggests that highly anisotropic Ln^{III} ions (i.e., Tb^{III} and Dy^{III}) are an essential contribution for the existence of an energy barrier for spin reversal.

Acknowledgment. We thank the DFG (CFN), MAGMANet (NMP3-CT-2005-515767), and Alexander von Humboldt Foundation (Y.-Z.Z.) for financial support and Rodolphe Clérac for helpful discussions.

Supporting Information Available: Experiments, crystal data (CIF file and additional structural data), and additional magnetic and synthetic data. This material is available free of charge via the Internet at <http://pubs.acs.org>.

IC9000686